PHYS 361 - Electronics Lab

Introduction to Data Acquisition

Jordan Ashley, Quintinne Madsen

February 18, 2025

1 Introduction

This lab explored the elements and utility of basic data acquisition, focusing on the interface between hardware and software components. This was accomplished via a graphical data acquisition programming environment and physical USB data acquisition system.

1.1 Terminology

- LabVIEW = Laboratory Virtual Instrument Engineering Workbench
- DMM = digital multimeter
- DAQ = data acquisition

1.2 Equations

- Thévenin voltage

$$V_{th} = V_{in} \cdot \frac{R_2}{R_1 + R_2} \tag{1}$$

- Thévenin resistance

$$R_{th} = (V_{th} - V_L) \cdot \frac{R_L}{V_L} \Rightarrow \frac{1}{R_{th}} = \frac{I_L}{V_{th} - V_L} \tag{2}$$

2 Methods

All data taken through the NI USB-6215 DAQ (Figure 1) used the NI MAX application program to connect the USB to the LabVIEW software through appropriate drivers, which were also configured by NI MAX.

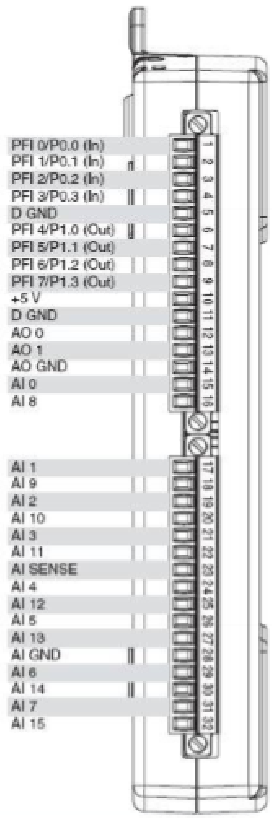

Figure 1: A diagram of the National Instruments USB-6215 data acquisition system, NI USB-6215 DAQ

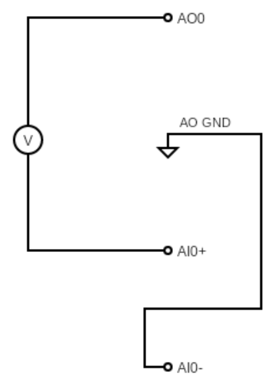

Figure 2: A diagram of the circuit used to measure the accuracy of voltage measurements

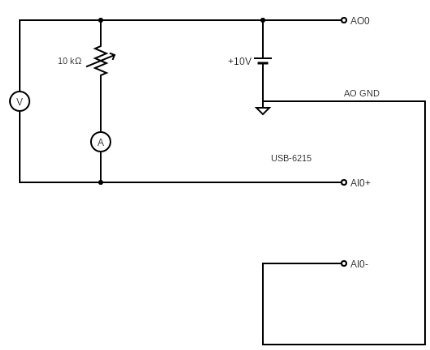

Figure 3: A diagram of the circuit used to measure the IV curve of the analog output source AO0

3 Results

3.1 Input-Output Characteristic

The difference between the output voltage reported by the DAQ, the voltage measured across AO0 and AI0+ as shown in Figure 2, and the voltage measured by the DAQ is very small. Figure 4 shows an overlay of the DAQ-reported output voltage against both the DMM (blue circles) and DAQ input (orange stars) voltage measurements, as well as the corresponding trendlines

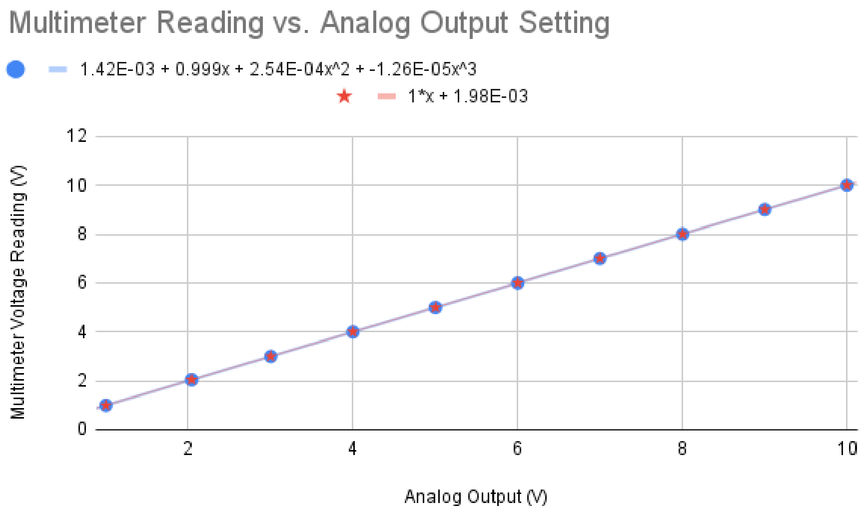

Figure 4: A plot of the DAQ reported output voltage versus voltage as measured using the circuit in Figure 2

and their equations. The equations reveal significant accuracy, with the DMM readings diverging by approximately 0.1%.

3.2 Load Curve of AO0

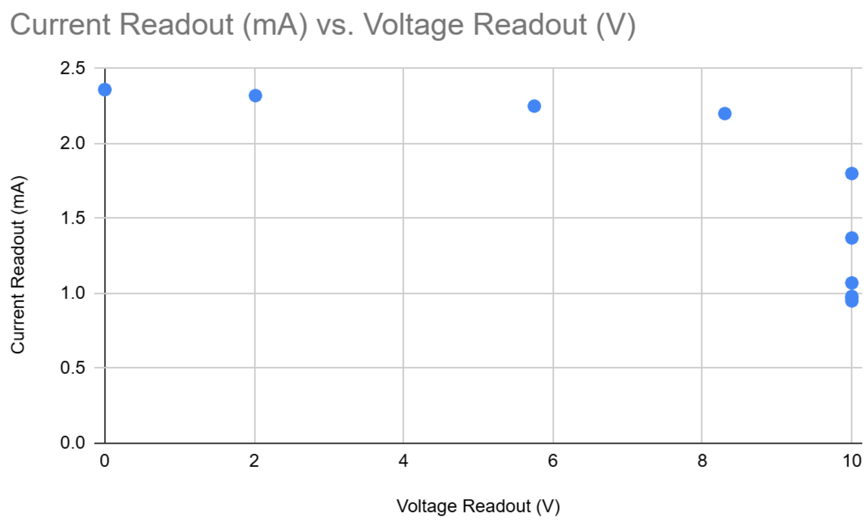

Figure 5: A plot of current versus voltage as measured using the circuit in Figure 3

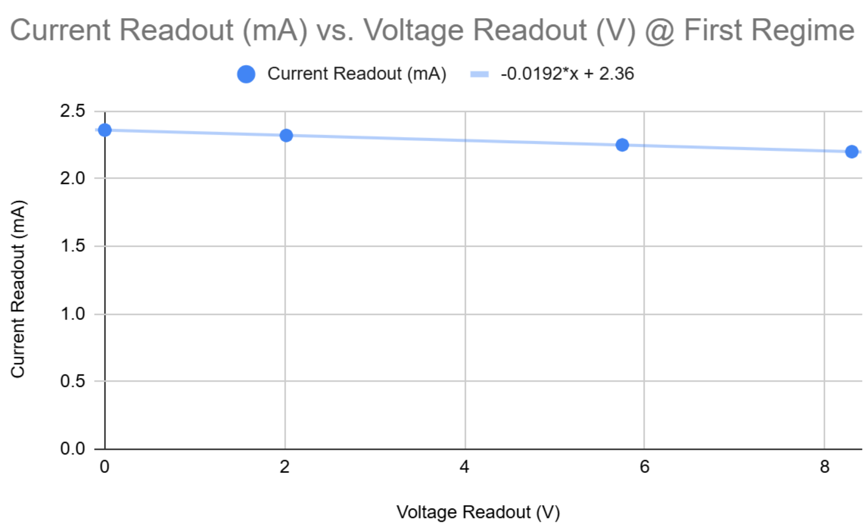

Figure 6: A plot of the first regime of the current versus voltage relationship as measured using the circuit in Figure 3

Figure 5 shows the relationship between current flowing through the 10 kΩ variable resistor and the voltage across it in the circuit shown in Figure 3. This plot reveals two separate regimes: an approximately linear relationship, where current gradually decreases with increasing voltage (Figure 6), and a sharp cutoff at 10 V, where the circuit begins to function like an ideal voltage source. From this, it can be concluded that the Thévenin voltage, V_{th}, is 10 V.

3.2.1 First Regime

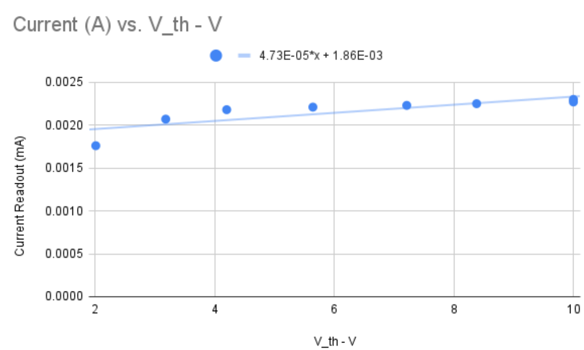

Figure 7: A plot showing the relationship between the measured current and the difference in the Thevenin voltage and the measured voltage

Equation 2 can be used with the equation for the trendline in Figure 7 to estimate the Thevenin resistance for the first regime, yielding

$$R_{th} = \frac{1}{4.73 \times 10^{-5}} \Omega = 21.1 \text{k}\Omega \tag{3}$$

This seems very high, and likely reveals an error in our current measurements.

3.2.2 Second Regime

The second regime models an ideal voltage source, which has a Thenevin resistance of 0.

3.3 Waveform Data

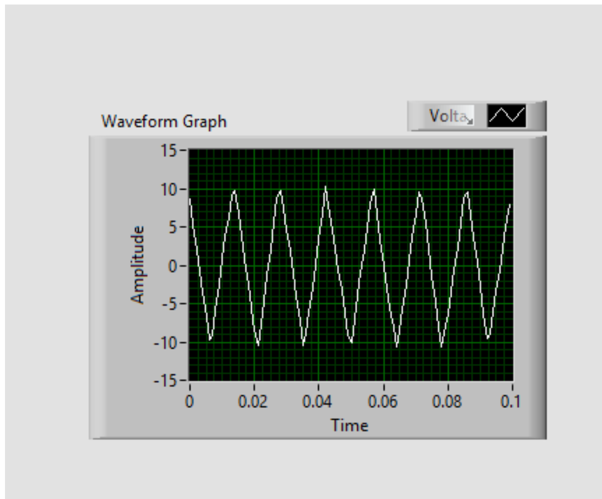

Figure 8: A screenshot of the DAQ output for the output of the function generator's sawtooth wave

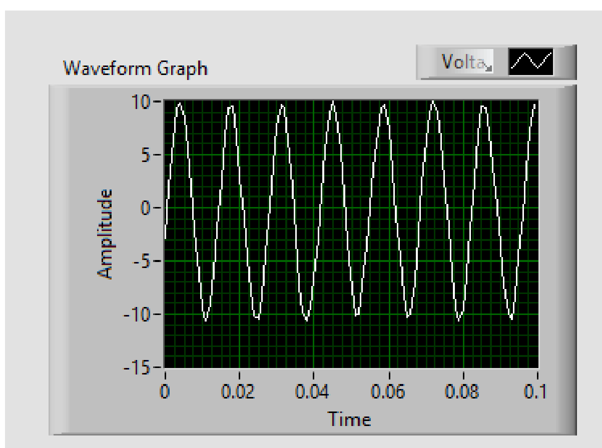

Figure 9: A screenshot of the DAQ output for the output of the function generator's sine wave

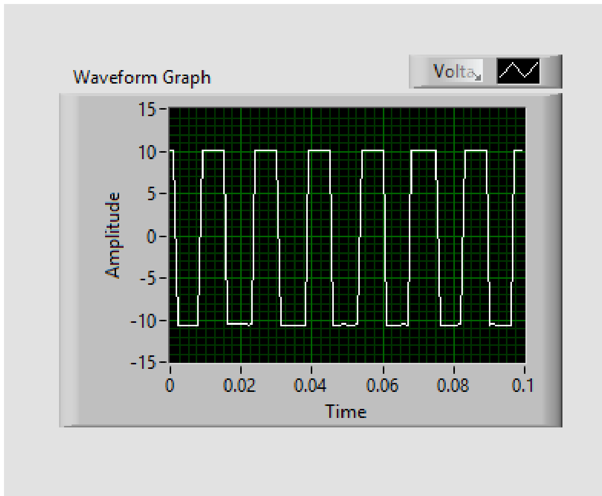

Figure 10: A screenshot of the DAQ output for the output of the function generator's square wave

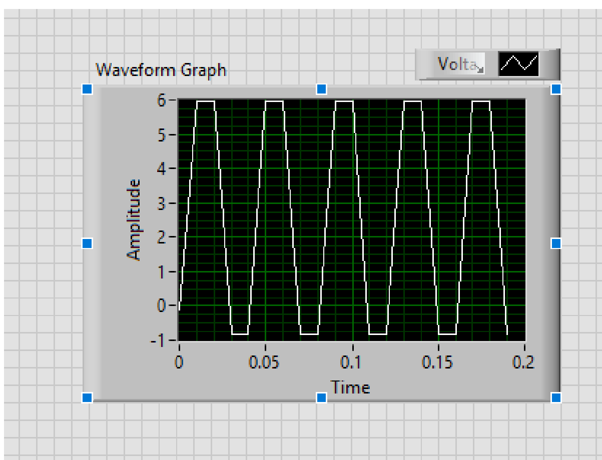

Figure 11: A screenshot of the DAQ output for the output of the function generator's square wave after applying a trigger

4 Conclusion

Our results demonstrated a high degree of accuracy in voltage measurements, with deviations of approximately 0.1% when comparing DAQ-reported values to DMM readings. These small discrepancies suggest that the DAQ measurements are reliable within acceptable tolerances. In the load curve of AO0, two distinct regimes were identified: an initial linear relationship where current decreases with increasing voltage and a second regime where that behaves like an ideal voltage source. The Thevenin voltage, estimated at 10V, aligns with expectations for the system, though the Thevenin resistance calculated in the first regime (Equation 3) is significantly higher than anticipated. This suggests a potential error in current measurements, which may have resulted from connection inconsistencies in the circuit used for this part of the lab (Figure 3). The waveform data collected from the function generator consisted of well-defined sawtooth, sine, and square wave outputs. The triggered square wave data confirmed that the DAQ system effectively synchronizes data capture, demonstrating its utility in capturing periodic signals with high precision. Overall, this experiment provided hands-on experience with data acquisition and the capabilities of the NI USB-6215 DAQ system. The results confirmed the accuracy of voltage measurements and the ability of the system to effectively characterize circuits and waveforms.